Spatiotemporal evolution and driving factors of carbon emissions in Qingdao City based on GeoDetector

Peifeng Zhang*, Yan Zhou, Kaiyuan Luan, Beibei Jia

College of Pipeline and Civil Engineering, China University of Petroleum, Qingdao 266580, China

Corresponding author: Peifeng Zhang, E-mail address: windzpf@163.com.

GRAPHICAL ABSTRACT

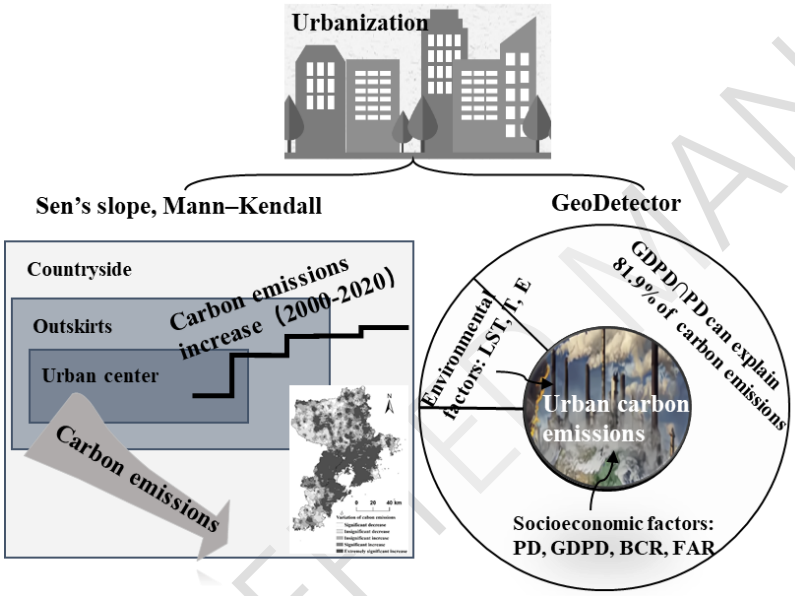

Abstract

Investigating the spatiotemporal characteristics and factors of urban carbon emissions is essential to reduce carbon emissions and achieve dual carbon goals. In this study, we examined the change tendency of carbon emissions using the coefficient of variation, the Sen's slope method, and the Mann–Kendall (MK) test and explored the effects of socioeconomic and environmental variables on

* Corresponding author. College of Pipeline and Civil Engineering, China University of Petroleum, Qingdao 266580, China
E-mail address: windzpf@163.com (P-F. Zhang).

carbon emissions using GeoDetector, in Qingdao City. The results revealed that: (1) From 2000 to 2020, carbon emissions increased annually, the area ratio of high carbon emissions increased and of low carbon emissions decreased yearly. Over 73% of carbon emissions have changed in a moderate way ($0.1< CV < 1$) and 80% of Qingdao City experienced an increased tendency ($\beta > 0$) in carbon emissions. (2) Carbon emissions diminished gradually from the urban center to the periphery. There were significant spatiotemporal disparities from one another in the subareas, Municipal districts had the largest variation degree (CV=0.32) and a huge growth trend of carbon emissions, while Laixi, Jiaozhou, and Pingdu were minor. (3) Socio-economic factors demonstrated a stronger ability to explain carbon emissions than environmental factors. GDP density, population density and floor area ratio were the key variables that affect the spatial distribution of carbon emissions, and the interaction between GDPD and PD can explain 81.9% of the carbon emissions in Qingdao. New technologies and materials, low-carbon energy consumption and lifestyles, and acceptable economic growth were the main strategies for Qingdao to become a low-carbon city.

Keywords: urban; carbon emissions; spatiotemporal evolution; socioeconomic factors; environmental factors; GeoDetector.

1. Introduction

In China, over 90% of carbon emissions are generated from metropolitan regions (He et al., 2019). It is crucial to investigate the spatiotemporal characteristics and factors of urban carbon emissions in order to reduce carbon emissions and achieve dual carbon goals. At national and regional scales, researchers analyzed the energy utilization, spatiotemporal variation characteristics, and influence factors of carbon emissions in Fujian Province (Wei and Chen, 2021), Yangtze River Delta region, and Qinghai Plateau (Liu and Zeng, 2021) based on DMSP/OLS data (Du et al., 2021), IPCC inventory method (Wang et al., 2019), panel data (Zhang and Pan, 2019), STIRPAT model (Shen et al., 2020), system dynamics method (Yang and Wu, 2021), U-Kaya and LMDI model (Wang et al., 2019), panel vector autoregression model (PVAR) (Zhao et al., 2021), and random forest (Liu et al.,

2019). They found considerable spatiotemporal disparities in carbon emissions, with economic development, energy consumption, industrial structure, population and technology being the main contributors. At the metropolitan scale, Xu et al. (2022) examined the spatiotemporal pattern of land use and carbon emissions using information entropy and Tapio model and found that there was spatiotemporal heterogeneity in the decoupling of urban land use and carbon emissions. Wang et al. (2020) detected the spatiotemporal features and driving factors of energy consumption and carbon emissions using the panel measurement method, in 158 cities, and found that urbanization and industrial structure have significant impacts on carbon emissions and energy consumption. Ma et al. (2021) analyzed the impact of urbanization on carbon emissions based on the entropy approach and geographically weighted regression (GWR) model (Wang et al., 2019). They found regional variations in the impact of population and urbanization on carbon emissions, with urbanization and economies contributing to the increase. Wang and Chen (2020) examined how urbanization affected carbon emission efficiency using the STIRPAT model and found that technology, GDP per capita, and information all had a positive impact on carbon emissions. Huo et al. (2021) detected the relationship between urbanization and buildings' carbon emissions based on the panel threshold regression and regression-enhanced random model (Zhang et al., 2021). They found that the impact of urbanization on building carbon emissions becomes more pronounced when per capita income and energy mix exceed a certain threshold. Population, economy, and technology were the key factors in building carbon emissions, which were positively correlated with per capita building area, energy intensity and have an inverted U-shape relationship with economic growth. Xu et al. (2021) analyzed the effect of urban three-dimensional structures on carbon emissions using the STIRPAT and ridge regression model, and found that building height and density were the primary factors driving the rapid growth of carbon emissions.

These studies focused on accounting for carbon emissions, their spatiotemporal characteristics, and the effects of socioeconomic, land use, and building-related variables. There is a paucity of analysis of the shifting trends in carbon emissions and the results of factor interactions. For the creation of

low-carbon development strategies, it is crucial to investigate the spatiotemporal change trends in carbon emissions during the urbanization process and to identify the influence factors and the effect of factor interactions on carbon emissions. The coefficient of variation has been utilized to disclose the variation features of time series data because it can reflect the relative variation of spatiotemporal data and eliminate the influence of scale and dimension (Liu et al., 2021). Sen's slope and Mann Kendal test have been frequently applied in trend analysis and testing studies of time series data (Ma et al., 2022) owing to their excellent calculation efficiency, insensitivity to measurement errors and outliers, independence from a particular distribution, and minimal interference from outliers (Ali et al., 2019). And GeoDetector was primarily used to investigate the impact of numerous elements on the spatiotemporal pattern (Pan et al., 2019) with its advantage of examining the spatial differentiation of geographical features, the explanatory power of factors, and detecting the interaction between factors (Zhou et al., 2020, Li et al., 2022).

From 2000 to 2020, the GDP and urban construction land increased by 10 and 6 times, respectively, in Qingdao City. Although annual carbon emissions have declined since the 11th Five-Year Plan due to the implementation of low-carbon development policies, the growth of total carbon emissions and urban environmental issues have become more prominent. The purpose of this paper aims to identify the evolutionary tendency of carbon emissions and investigate the effects of socioeconomic and environmental factors on carbon emissions using the coefficient of variation, Sen's slope trend, Mann-Kendall test, and GeoDetector, in Qingdao City.

2. Study area

Qingdao is a rapidly developing city in Shandong Province, China, with a total area of 11293 km^2. It consists of 7 municipal districts (Shinan, Shibei, Licang, Laoshan, West Coast New Area, Chengyang, and Jimo) and 3 county-level cities (Jiaozhou, Pingdu, and Laixi), with areas of 5226 km^2 and 6067 km^2, respectively. The municipal districts have a long history of urbanization, high socioeconomic growth and urbanization levels, and a concentrated population, economy, and industry. Its elevation ranged from 0 to 1090 meters, mountains account for 17.6% of the total area and are located in the

southeast and north of the city, while plains and basins account for 59.4% of the entire city (Figure 1). It has experienced significant changes in industrial structure, construction landscape, and the ecological environment resulting from socioeconomic development and urban renewal policies from 2000 to 2020. GDP rose to 1240.06 billion yuan from 118.31 billion yuan, with the ratio of the secondary industries falling to 35.2% from 46.1% and the tertiary industries rising to 19%. Both the urban built-up area and population increased by 639.1km^2 and 2939.2 thousand, separately (Qingdao Municipal Bureau of Statistics, 2021). The implementation of low-carbon development policies from 2006 resulted in a 45% reduction in carbon emissions per unit of GDP from 2005 to 2020. However, the general amount of carbon emissions is on the rise, and socioeconomic development considerably affects the spatiotemporal heterogeneity of those emissions.

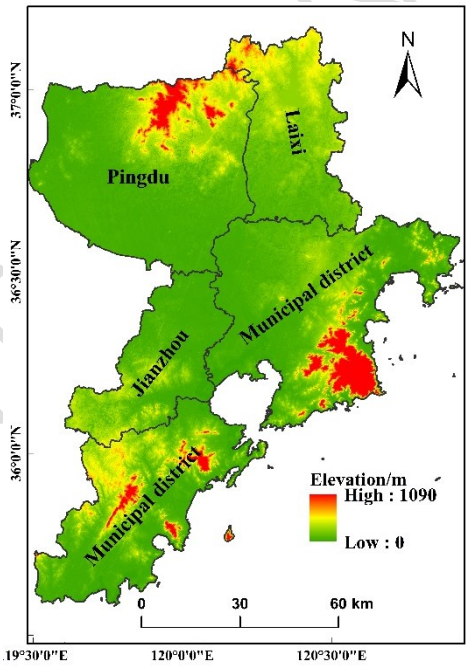

Figure 1. The study area

3. Materials and Methods

We detected the change characteristics of carbon emissions and explored the effects of socioeconomic and environmental factors on carbon emissions from 2000 to 2020, in Qingdao City. The flowchart of the applied methodology in the research is shown Figure 2.

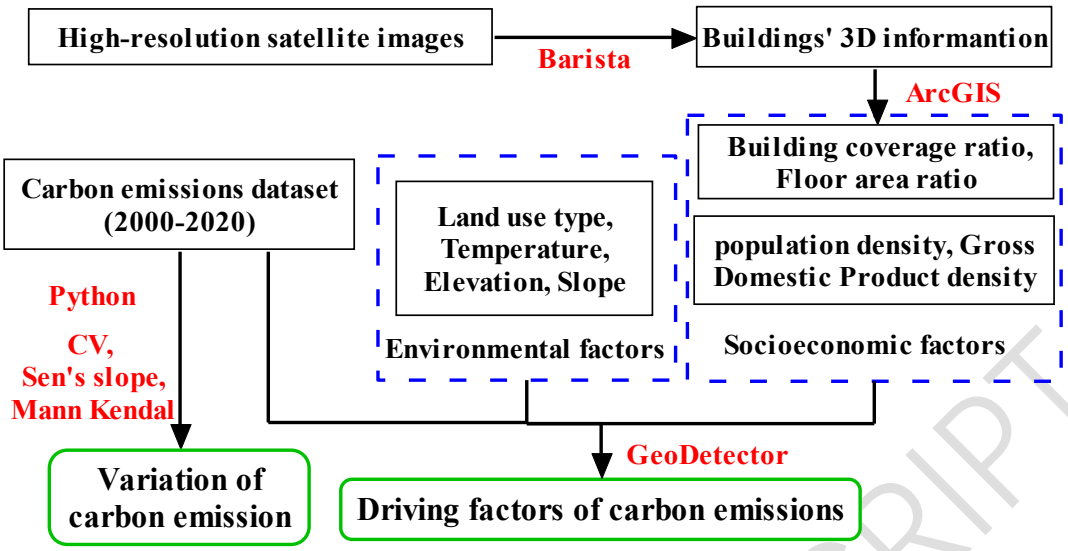

Figure 2. The flowchart of methodology

3.1. Data collection

A time series raster data in Qingdao with a resolution of 1km×1km from 2000 to 2020 attained as follows: the carbon emissions data of fossil fuels attained from the ODIAC fossil fuel emission dataset (https://db.cger.nies.go.jp/dataset/ODIAC/). Annual average temperature data were from National Earth System Science Data Center (https://www.geodata.cn/). Land use and GDP density data were from the Resource and Environmental Science and Data Center (https://www.resdc.cn/DOI/doi.aspx?DOIid=33). Population density data were from the World population dataset (https://www.worldpop.org/geodata/listing?id=76). The 30m × 30m resolution digital elevation model was obtained from the Geospatial data cloud(https://www.gscloud.cn/sources/). Buildings' 3D information (buildings' frame and height) was extracted from high-resolution satellite images using the monoplotting function of Barista software, a manual method mainly based on the Digital Elevation Model, Ground Control Points and a set of Rational Polynomial Coefficients (Zhang et al., 2014). The height accuracy of buildings extracted by Barista is 91.8% (Zhang, 2015) based on buildings that were randomly measured in the field. ArcGIS was used to calculate the floor area ratio and building coverage ratio. And the building coverage ratio and floor area ratio were calculated using ArcGIS.

3.2. Data pre-processing

The land use type (LST) was divided into 8 categories according to the composition of land use in the study area and the purpose of the study. The population density (PD, thousand people/km^2), Gross Domestic Product density (GDPD, million yuan/km^2), Building coverage ratio (BCR, %), Floor area ratio (FAR), Average temperature (T, ℃), Elevation (E, m) and Slope (S, °) were each divided into 9 groups by natural breakpoint method (Ma et al., 2022) (Table 1). All the data were retrieved using 10742 grids with a resolution of 1km×1km, in Qingdao City.

Table 1. Classification of environmental and socioeconomic factors

Types	Environmental factors				Socioeconomic factors			
	T (℃)	S (°)	E(m)	LST	PD (thousand people/km^2)	GDPD (million yuan/km^2)	BCR (%)	FAR
1	8.9-10.4	0-2.23	0-26	CL	0-0.1	1.52-21.03	0-2.74	0-0.05
2	10.4-10.9	2.23-4.97	26-56	F	0.1-0.3	21.03-30.28	2.74-8.23	0.05-0.16
3	10.9-11.5	4.97-8.20	56-94	W	0.3-0.7	30.28-47.10	8.23-15.29	0.16-0.31
4	11.5-12.1	8.20-11.92	94-149	RL	0.7-1.2	47.10-70.29	15.29-23.92	0.31-0.53
5	12.1-12.6	11.92-16.40	149-231	UL	1.2-1.9	70.29-113.77	23.92-34.50	0.53-0.85
6	12.6-13.0	16.40-21.62	231-342	GL	1.9-3.0	113.77-258.17	34.50-47.45	0.85-1.40
7	13.0-13.3	21.62-27.58	342-486	UC	3.0-4.2	258.17-554.58	47.45-61.17	1.40-2.19
8	13.3-13.6	27.58-35.28	486-690	R	4.2-5.9	554.58-1066.55	61.17-75.29	2.19-3.22
9	13.6-14.2	35.28-63.37	690-1088		5.9-8.3	1066.55-9337.56	75.29-100	3.22-4.82

Note: Cultivated land (CL); Forest (F); Water (W); Rural construction land (RL); Unused land (UL); Grassland (GL); Urban construction land (UC); Roads (R).

3.3. Calculation method for carbon emission variation

The variation of carbon emissions in Qingdao was analyzed using the coefficient of variation, Sen's slope method, and the Mann Kendal test based on Python. The coefficient of variation (CV) was used to estimate the relative variance in carbon emissions from 2000 to 2020, which can be derived as indicated in Equation (1):

$$CV = \sigma/\mu \quad (1)$$

Where σ is the standard deviation of carbon emissions, unit (t); μ is the average value of carbon emissions. When CV<=0.1 means weak variation, CV>=1 means strong variation, and 0.1<CV<1 means moderate variation.

Sen's slope is a non-parametric method for evaluating the propensity to change in time series data and has been shown to be quite reliable. It was used to estimate trends in carbon emissions from 2000 to 2020. And according to Equation (2), Sen's slope (β) is a median of all the slopes that calculated all the subsequent data points of a time series carbon emission.

$$\beta = median\left((CE_j - CE_i)/(j - i)\right) \quad (2)$$

Where CE_i and CE_j represent the carbon emissions in i and j years, 1<i<j<n; β >0 and β <0 indicated that the carbon emissions are increasing and decreasing, respectively.

Mann–Kendall test is recommended by the World Meteorological Organization as the most popular test because it considers the data distribution and eliminates outliers. Mann–Kendall test (Z) was used to gauge the significance of the variation in carbon emissions, as shown in Equation (3), The value of Z indicates the direction of the trend. A value of minus Z indicates a decreasing trend and vice versa. If the absolute value of Z exceeds 1.64, the significance test is passed with 90% confidence and the value is significant at the 10% level. If the absolute value of Z is higher than 1.96, the significance test is passed with 95% confidence, and the value is significant at the 5% level. The significance level (P): 0.05<P<0.1 denotes a significant increase or decrease, and P<0.05 denotes an extremely significant increase or decrease.

$$\begin{cases} Z = (S-1)/\sqrt{Var(S)}, & S > 0 \\ Z = 0, & S = 0 \\ Z = (S+1)/\sqrt{Var(S)}, & S < 0 \end{cases} \quad (3)$$

Where S is the test statistic for carbon emissions (Ali et al. 2019).

3.4. Detecting driving factors of carbon emissions based on GeoDetector

GeoDetector is a set of statistical methods to detect spatial distinction and identify the driving force (Wang and Chen, 2017). Factor detector (q) was used to detect the impact of socioeconomic and environmental factors on the carbon emissions' distribution, and the q-statistic can be generated from Equation (4). The value of q is strictly within [0, 1], q=1 indicates that the factor (X) fully determines the spatial distribution of carbon emissions; q=0 denotes that there is no relationship between the factor (X) and carbon emissions. The larger value of q means the factor (X) has a greater influence or stronger explanatory power on carbon emissions.

$$q = 1 - (\sum_{h=1}^{L} N_h \sigma_h^2)/N\sigma^2 \quad (4)$$

Where N is the number of samples in the study area; L is the number of factor layers; h is the number of argument layers, h∈[1, L]; $\sigma^2$is the variance of the dependent variables.

Interaction detector was used to evaluate whether the factors (X) interacting with one another will weaken or enhance the explanatory power of the dependent variable (Y), or whether these factors (X) are independent and their interaction has no impact on the dependent variable (Y). And the q-statistic divides the explanatory power of factors(X) to the dependent variable (Y) into 5 intervals (Table 2). The interactive explanatory power of socioeconomic and environmental factors to the carbon emissions was detected in Qingdao City.

Table 2. Interaction between explanatory variables (Xs)

Description	Interaction
$q(X1 \cap X2) < Min(q(X1), q(X2))$	Weaken, nonlinear
$q(X1 \cap X2) = q(X1) + q(X2)$	Independent
$Min(q(X1), q(X2)) < q(X1 \cap X2) < Max(q(X1), q(X2))$	Weaken, uni-, nonlinear
$q(X1 \cap X2) > q(X1) + q(X2)$	Enhance, nonlinear
$q(X1 \cap X2) > Max(q(X1), q(X2))$	Enhance, bi-

Ecological detector was used to identify the differences between the two factors in carbon emissions. It is measured by the F-statistic and can be calculated in Equation (5). At the significance level of

0.05, the result was expressed as 'T' means there was a significant difference between the effects of one factor (X1) and another factor (X2) on the dependent variable (Y), and the result was expressed as 'N' means there was no difference existed.

$$F = (N_{X1}(N_{X2} - 1)SSW_{X1})/(N_{X2}(N_{X1} - 1)SSW_{X2})$$

$$SSW_{X1} = \sum_{h=1}^{L1} N_h \sigma_h^2 x, \quad SSW_{X2} = \sum_{h=1}^{L2} N_h \sigma_h^2 x \tag{5}$$

Where N_{X1} and N_{X2} are the sample sizes of the factors; SSW_{X1} and SSW_{X2} are the sums of the variances in the argument layer; L1 and L2 are the number of layers; h is the number of argument layers, $h \in [1, L]$; σ^2 is the variance of the dependent variables.

4. Results and Discussion

4.1. Spatiotemporal characteristics of carbon emissions

The carbon emissions increased yearly due to the socioeconomic development in Qingdao, which is similar to the earlier research (Zheng et al., 2020). The average, maximum, and standard deviation (SD) of carbon emissions varied significantly from 2000 to 2020, in Qingdao (Figure 3). Rapid development of the population, economy, and secondary industry is the main driving force of this status.

From 2000 to 2005, the maximum and SD of carbon emissions increased more quickly than the average value, and they increased by 15.93 $\times 10^4$t/a, 1700t/a, and 40t/a, separately. GDP and secondary industries grew by 34.24 billion yuan/a and 42.26 billion yuan/a, respectively, urban land expanded from 119.1 km^2 to 178.8 km^2, and more high-carbon emitting companies were established, all contributing to the rapid growth of carbon emissions and variability characteristics. From 2005 to 2015, the average, maximum, and SD of carbon emissions increased smoothly, increasing by 20t/a, 4.82$\times 10^4$t/a, and 390t/a due to the steady growth of population, industry, GDP, and urban land (increased by 2 million population/a, 9.4 billion yuan/a, 60 billion yuan/a, and 38.8 km^2/a, respectively). From 2015 to 2020, both the maximum and the SD of carbon emissions were growing

slowly, while the average carbon emissions were increasing rapidly at a rate of 160t/a, which is four times higher than in 2000-2005 and eight times higher than in 2005-2015. The structural optimization of industry and energy, the implementation of energy policies, and the rapid socioeconomic development have contributed to the changing character of carbon emissions during this period.

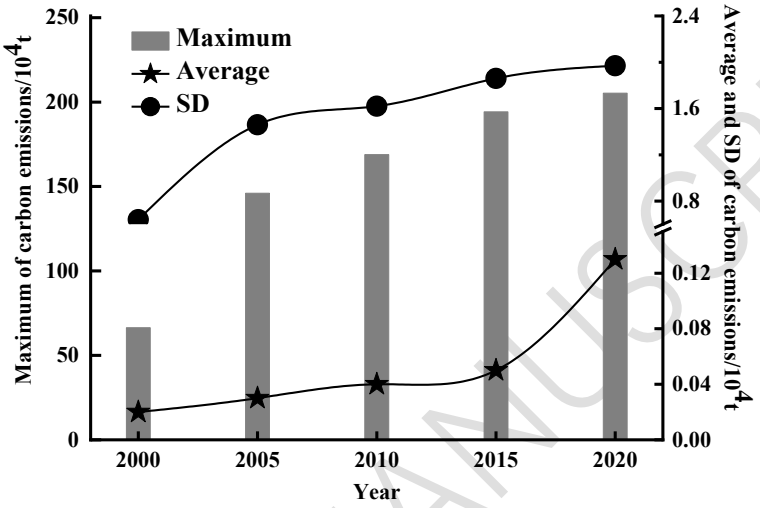

Figure 3. Carbon emissions in Qingdao City

Figure 4 has shown that the area ratio of higher carbon emissions increased and of lower carbon emissions decreased yearly, and that carbon emissions gradually reduced from the urban centers to the periphery. From 2000 to 2020, most of the carbon emissions above 2000t/km^2 were concentrated in urban centers, with their area ratio increasing from 3% to 12%. Carbon emissions in the 400-2000t/km^2 range were located around urban centers, with the area ratio increasing from 9% to 25%. Carbon emissions in the 200-400t/km^2 range and below 200t/km^2 were mainly in the urban periphery, where the area proportion reduced from 43% to 37% and 45% to 26%, respectively. Most of the carbon emissions below 200t/km^2 were discovered in forests, grasslands, farms and mountains. Disparities in land use, economy and population were the primary determinants of the spatiotemporal heterogeneity in carbon emissions in Qingdao. The population, economy, industry, transport and energy consumption were concentrated in urban centers, which had the highest and fastest increase in carbon emissions. The density of population, economy, energy consumption and carbon emissions

were gradually reduced from the urban centers to the periphery. Forests, grasslands and mountains had the lowest carbon emissions. The increase in population, urban construction, GDP and energy consumption contributed to the increase in carbon emissions in the study area from 2000 to 2020.

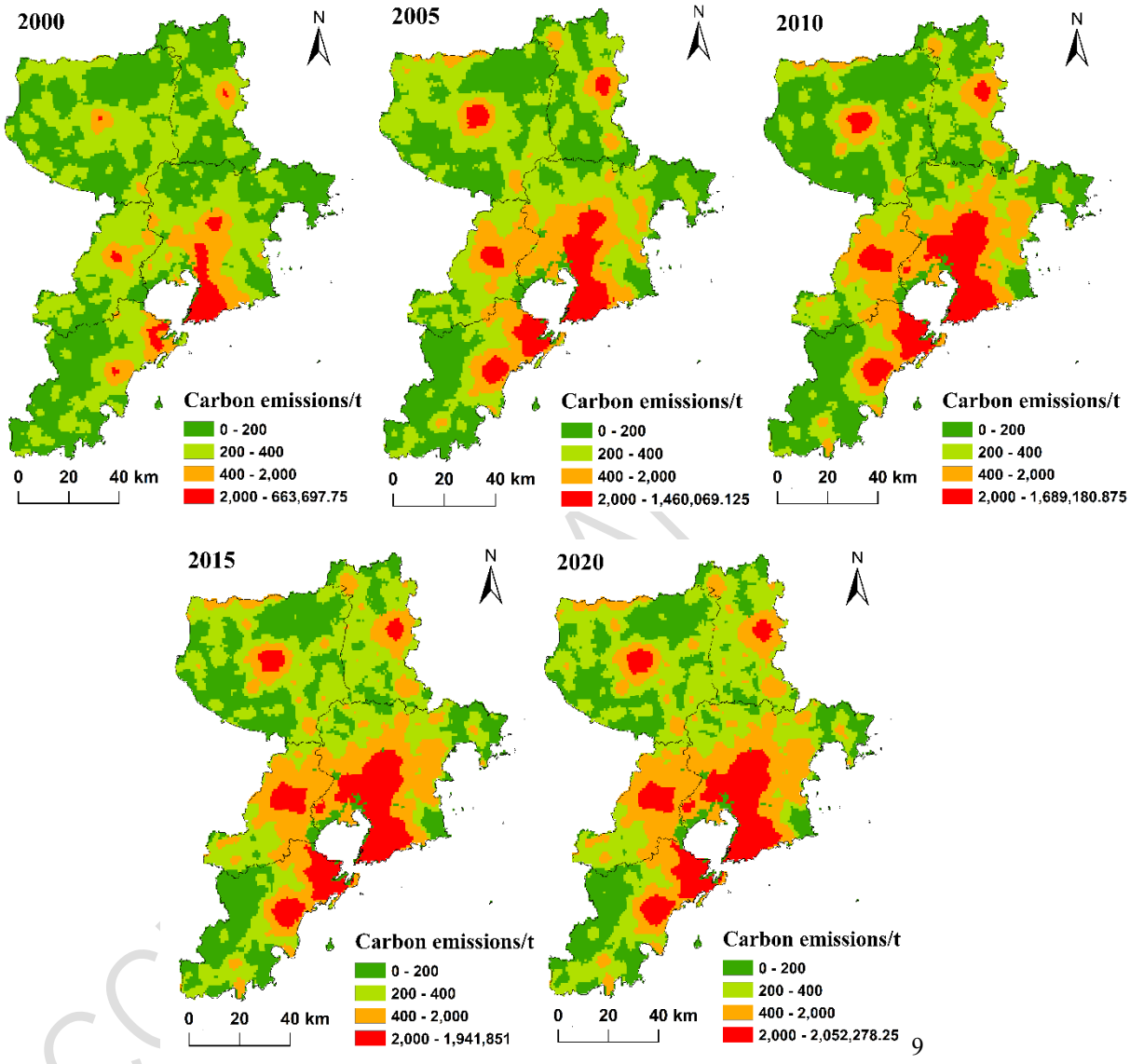

Figure 4. Distribution of carbon emissions

4.2. Spatio-temporal distinction of carbon emissions among subareas

The composition and variation of carbon emissions varied significantly from one another in the subareas (Pingdu, Laixi, Jiaozhou, and Municipal districts) (Figure 5) due to the diversity of urbanization, economic patterns, industrial structure, which is similar to the earlier research (Wang et

al. 2020). Generally, the area ratio of carbon emissions increased above 400t/km^2 and decreased below 400t/km^2, in these subareas, from 2000 to 2020. Compared with these subareas, the largest proportion and the fastest growth rate of carbon emissions were in Municipal districts above 2000t/km^2. Jianzhou noticed the fastest rise (41.1%) and decline (29.4%) in carbon emissions in 400-2000t/km^2 and 200-400t/km^2, respectively. The largest reduction (38.6%) in carbon emissions below 200t/km^2 was found at Laixi. The majority of carbon emissions below 400t/km^2 were produced in Pingdu (>85%) and Laixi (>75%).

From 2000 to 2020, Municipal districts' carbon emissions raised from 6.3% to 21% above 2000t/km^2 and from 13.9% to 28.1% in the 400-2000t/km^2 range, and declined from 36.6% to 26.5% in the 200-400t/km^2 range and from 43.1% to 24.3% below 200t/km^2, respectively. Jiaozhou's carbon emissions raised from 1.1% to 10.4% above 2000t/km^2, primarily manifested as a rapid increase (41.1%) in the 400-2000t/km^2 range and decrease (29.4%) in the 200-400t/km^2 range. Laixi's carbon emissions were reported to be declining rapidly below 200t/km^2 and growing at roughly equal rates in the 400-2000t/km^2 and 200-400t/km^2 ranges. Pingdu's carbon emissions were expressed as a decrease below 200t/km^2 and an increase in the range of 400-2000t/km^2.

Population, economy, policy, industrial structure, energy consumption, and the phase of urban growth were the key determinants of the variation in carbon emissions in the subareas. Municipal districts acted as the political, economic, cultural and trade hubs of Qingdao. It has experienced rapid socio-economic development and has the largest carbon emissions and the fastest growth rate compared to other sub-areas. Since 2005, many high-emission enterprises have relocated to Jiaozhou from Municipal districts, which coincided with the rapid growth of the population and economy, leading to a sharp rise in carbon emissions. Laixi and Pingdu had a tiny amount of land used for urban construction, a modest economy, and a declining population. However, they had a substantial quantity of land used for farming, forestry, grassland, and rural construction, all of which made them maintain lower carbon emissions.

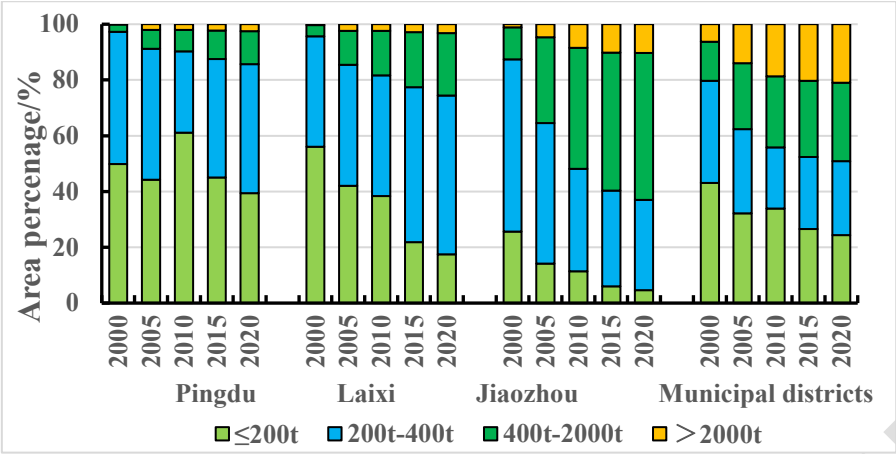

Figure 5. Area percentage of carbon emissions in subareas

4.3. The variation tendency of carbon emission

The CV of carbon emissions ranged from 0.06 to 2, with weak variation (CV<=0.1), moderate variation (0.1<CV<1), and strong variation (CV>=1) accounting for 22.6%, 73.8%, and 3.6% of the whole research area, respectively. The majority of Qingdao's carbon emissions have changed in a moderate way over the last 20 years. Weak variation, moderate variation, and strong variation were distributed in the village and agricultural regions, urban areas, and forestry and grassland, correspondingly (Figure 6). Municipal districts in possession of moderate variation and strong variation over 45%, separately, and Pingdu accounted for over 48% of the weak variation and strong variation, respectively (Table 3).

Carbon emissions differed significantly from one another in the subareas. Municipal districts (CV=0.32) had the greatest degree of variation in carbon emissions, while Laixi (CV=0. 2) had the least. Moderate variation accounts for 81.7%, 90.4%, 72.1%, and 56.2% of areas in Municipal districts, Jiaozhou, Laixi, and Pingdu, respectively, while Laixi and Pingdu both have over 26% of areas with weak variation. Various types of land-use were the primary cause of the distinct variation in carbon emissions.

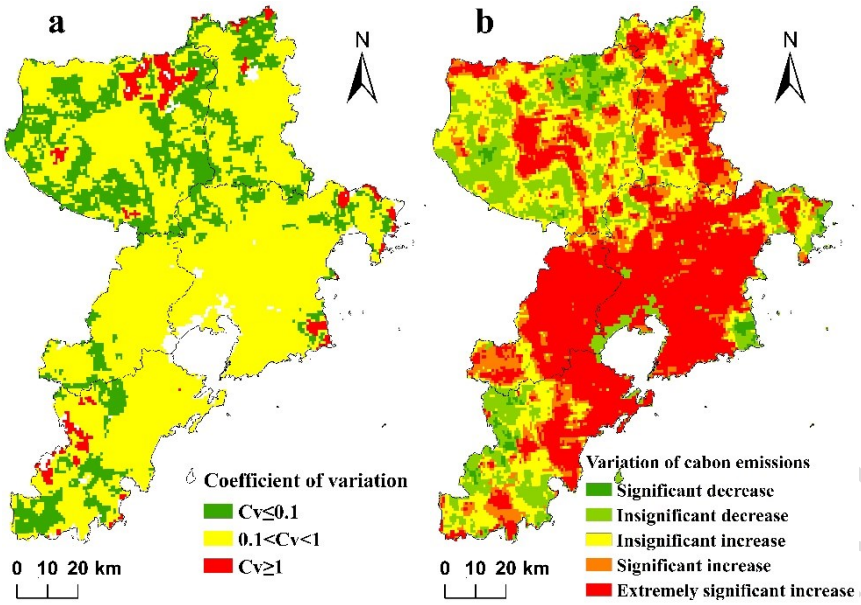

Figure 6. Distribution of coefficient of variation (a) and variation of carbon emissions (b) from 2000 to 2020

From 2000 to 2020, over 80% of Qingdao City experienced an increased tendency (β>0) in carbon emissions, and they were primarily concentrated in urban areas. Additionally, a significant increase in carbon emissions was detected across 56% of the study region (Table 3). Agricultural, forestry, and grassland zones showed a decreased tendency in carbon emissions (Figure 5). Municipal districts were responsible for 37.2% of carbon emissions with an increased tendency (β>0) and 8.1% with a decreased tendency (β<0). Pingdu, Laixi, and Jiaozhou accounted for 19%, 13.3%, and 11.3% of carbon emissions with an increased tendency (β>0), respectively.

Carbon emissions have risen sharply over the past two decades in Qingdao. Municipal districts exhibited an increasingly evident upward tendency in carbon emissions, followed by Pingdu. The differences in carbon emissions were remarkably compatible with the spatial-temporal disparities in socioeconomic development and land-use patterns in the subareas.

Table 3. Area percentage of CV and variation tendency for carbon emissions in subareas (%)

Subarea	CV			β<0		β>0		
	CV<=0.1	0.1<CV<1	CV>=1	P<0.05	-	0.05<P<0.1	P<0.05	-
PingDu	49.4	22.4	48.6	1.1	8.7	3.8	4.3	10.9
LaiXi	16.8	14.1	6.8	0.1	0.8	3.6	5.3	4.4

JiaoZhou	5.0	14.4	0.0	0.0	0.4	1.8	8.5	1.0
Municipal districts	28.8	49.1	44.6	0.9	7.2	5.4	24.3	7.5
Total	100	100	100	2.1	17.1	14.6	42.3	23.9

Note: P<0.05, extremely significant; 0.05<P<0.1, significant; —, insignificant.

4.4. The driving factors of carbon emissions

The influence degree of factors on carbon emissions was calculated using the factor detector, and the q-statistic of all factors ranged from 0.003 to 0.728 (Table 4), the explanatory power of factors on carbon emissions, with GDPD > PD > FAR > T > BCR > E >LST > S is a descending order. In comparison to natural environmental factors, socio-economic factors (GDPD, PD, and FAR) demonstrated a stronger ability to explain carbon emissions. It is on par with the results of a previous research paper, which found that an inverted U-shaped link between GDP and carbon emissions meets the Kuznets curve (Wang and He, 2019), population, technology, and urban economic growth all had positive correlations with carbon emissions, whereas temperature and precipitation had negative correlations (Li et al., 2019). Inhabitants and buildings are the main components of a city and account for the bulk of energy consumption for daily activities and urban development. Thus, GDP density, population density, and floor area ratio were Qingdao's most important and powerful explanatory indicators of carbon emissions over the last two decades.

Table 4. Q-statistic of the factor detector

	T	S	E	LST	PD	GDPD	BCR	FAR
q-statistic	0.074	0.003	0.006	0.005	0.595	0.728	0.039	0.553
Significance	0	0	0	0	0	0	0	0

The results of the interaction detector (Table 5) have demonstrated that a combination of socioeconomic and environmental factors has a larger effect on carbon emissions than either factor has on its own. The interaction between GDPD and PD, FAR, BCR, and T presented a double-factor enhancement in their explanatory power, with the order of the explanatory power being GDPD∩PD (81.9%)>GDPD∩FAR(79.4%)>GDPD∩BCR(75.5%)>GDPD∩T(74.2%)>PD∩FAR(72.3%)>PD∩T(61.4%). The interaction of other factors was a nonlinear enhancement, with environmental factors

interacting with GDPD, PD, FAR and BCR accounting for more than 70%, 62%, 56% and less than 10% of the spatial differences in carbon emissions, respectively. The interaction of GDPD, PD, and FAR with the rest of the factors can enhance the explanatory power of spatial differences in carbon emissions. In particular, the interaction between GDPD and PD had an explanatory power of 81.9% for the carbon emissions in Qingdao.

Table 5. Results of the interaction detector and the ecological detector

Indexes	T	S	E	LST	PD	GDPD	BCR	FAR
T	0.074	N	N	T	T	N	N	T
S	0.079	0.003	N	T	T	N	T	T
E	0.082	0.011	0.006	T	T	N	T	T
LST	0.098	0.012	0.014	0.005	T	N	N	N
PD	0.614*	0.667	0.622	0.634	0.595	N	N	N
GDPD	0.742*	0.740	0.737	0.754	0.819*	0.728	T	T
BCR	0.175	0.051	0.048	0.054	0.717	0.755*	0.039	T
FAR	0.566*	0.592	0.601	0.586	0.723*	0.794*	0.647*	0.553

Note: ___is a nonlinear enhancement, and * is a double-factor enhancement. T denotes that $Y(X_i)$ was a significant difference from $Y(X_h)$, while N expresses the opposite meaning.

The statistically significant differences between factors discovered by the ecological detector (Table 5) have shown that there were significant differences between PD and environmental factors, GDPD and socioeconomic factors (BCR, FAR), BCR and environmental factors (S, E), LST, FAR and environmental factors (T, S, E). Other factors did not significantly differ from one another in their impact on carbon emissions.

Generally, compared with the natural environment, socio-economic factors were the main drivers of Qingdao's carbon emissions from 2000 to 2020. GDP density, population density, and floor area ratio were the most powerful explanatory indicators for carbon emissions.

This study solely uses Qingdao as a sample in order to investigate the spatiotemporal variation characteristics of carbon emissions during the last 20 years due to the limits of spatiotemporal data gathering. Regional restrictions apply to the changing features and spatiotemporal variations of carbon emissions in Qingdao, but they also perfectly encapsulate those of the majority of Chinese cities. In order to identify the general characteristics of urban emissions in China, the national scale

and longer time series data are required. Only the primary elements from the natural environment and socio-economic factors are chosen for analysis of the carbon emission factors due to data limitations, and the identification of factors has certain restrictions. Similar to the findings of other studies, socio-economic factors have a large impact on urban carbon emissions. For the carbon emissions in Qingdao, the interaction between GDPD and PD has an explanatory power of 81.9%. This value must be verified by the analysis of multi-city, large-scale spatial, and longer time series datasets because of the limitations of time and space scale. The results of this study will offer guidelines for the development of low-carbon cities.

5. Conclusion

This study examined the spatiotemporal differences and driving factors of carbon emissions in Qingdao City from 2000 to 2020 using the coefficient of variation, Sen's slope, the Mann-Kendall test, and GeoDetector. The following conclusions are drawn: (1) Annual increases in carbon emissions and the area ratio of high emissions have been seen in Qingdao City for the previous 20 years. (2) Regional variances were apparent in carbon emissions. Carbon emissions were gradually reduced from the city center to the periphery. Municipal districts had the largest carbon emissions and the highest growth rates. (3) Socio-economic factors provided the strongest explanatory power for carbon emissions, particularly GDP density, population density, and floor area ratio. The interaction between GDPD and PD can explain 81.9% of the distribution in carbon emissions, whereas the effect of the natural environment factors was negligible. (4) New building energy-saving technologies and materials, low-carbon energy consumption and lifestyles, appropriate economic and population growth, and new technologies were the major strategies for the low-carbon city in Qingdao.

Declaration of Competing Interest

The authors declare that they have no known competing financial interests or personal relationships that could have appeared to influence the work reported in this paper.

Acknowledgments

This work was supported by the Key Project of the Shandong Province Natural Science Foundation (No. ZR2018QD001), National Natural Science Foundation of China (No. 41301198) and Fundamental Research Funds for the Central Universities (No. 18CX02078A).

References

Ali, Kuriqi, Abubaker and Kisi. (2019), Long-Term Trends and Seasonality Detection of the Observed Flow in Yangtze River Using Mann-Kendall and Sen's Innovative Trend Method, *Water,* **11**, 1-17. https://doi.org/10.3390/w11091855

Du H.B., Wei W., Zhang X.Y. and Ji X.P. (2021), Spatio-temporal evolution and influencing factors of energy-related carbon emissions in the Yellow River Basin: Based on the DMSP/ OLS and NPP/VIIRS nighttime light data, *Geographical research*, **40**, 2051-2065.

He C., Jiang K., Chen S., Jiang W. and Liu J. (2019), Zero CO_2 emissions for an ultra-large city by 2050: case study for Beijing, *Current Opinion in Environmental Sustainability*, **36**,141-155. https://doi.org/10.1016/j.cosust.2018.10.006

Huo T., Cao R., Du H., Zhang J., Cai W. and Liu B. (2021), Nonlinear influence of urbanization on China's urban residential building carbon emissions: New evidence from panel threshold model, *Science of the Total Environment,* **772,**1-11. https://doi.org/10.1016/j.scitotenv.2021.145058

Li J.B., Huang X.J., Sun S.C. and Chuai X.W. (2019), Spatio-temporal coupling analysis of urban land and carbon dioxide emissions from energy consumption in the Yangtze River Delta region, *Geographical research*, **38**, 2188-2201.

Li Y., Zhang G.Q., Lin T., Ye H., Liu Y.Q., Chen T.Y. and Liu W.H. (2022), The spatiotemporal changes of remote sensing ecological index in towns and the influencing factors: A case study of Jizhou District, Tianjin. *Acta ecologica sinica*, **42**, 474-486.

Liu F. and Zeng Y.N. (2021), Analysis of the spatio-temporal variation of vegetation carbon source /sink in Qinghai Plateau from 2000—2015, *Acta ecologica sinica*, **41**, 5792-5803.

Liu W.D., Tang Z.P., Xia Y., Han M.Yand Jiang W.B. (2019), Identifying the key factors influencing Chinese carbon intensity using machine learning, the random forest algorithm, and evolutionary

analysis, *Acta geographica sinica*, **74**, 2592-2603.

Liu Y.M., Gu J.L., Zhang Z.Y., Liu Q. and Li G.C. (2021), Research on the spacial heterogeneity of regional social identity based on geographical detector, *Geographical research*, **40**, 495-512.

Ma M.Y., Zheng J.W. and Ma, T. (2021), Spatiotemporal characteristics of the impact of new urbanization on China's carbon dioxide emissions from a multi-dimensional perspective, *Acta Scientiae Circumstantiae*, **41**, 2474-2486.

Ma X.N., Ren Z.P., Xie M.Y., Li Z.B., Li P. and Zhang X. (2022), Quantitative analysis of environmental driving factors of vegetation coverage in the Pisha sandstone area based on geodetector, *Acta ecologica sinica*, **8**, 1-11.

Pan H.Y., Huang P. and Xu J. (2019), The spatial and temporal pattern evolution of vegetation NPP and its driving forces in middle-lower areas of the Min River based on geographical detector analyses, *Acta ecologica sinica*, **39**, 7621-7631.

Qingdao Municipal Bureau of Statistics, NBS Survey Office in QingDao, (2021), Qingdao. Statistical Yearbook, Beijing: China Statistics Press, 2021.

Shen Y., Wang C.C., Gao, C. and Ding L. (2020), Spatio-temporal distribution and its influencing factors of carbon emissions in economic zone of Zhejiang Bay Area based on urbanization, *Journal of Natural Resources*, **35**, 329-342.

Wang J.F. and Xu C.D. (2017), Geodetector: Principle and prospective, *Acta geographica sinica,* **72**, 116-134.

Wang L., Pei J., Geng J. and Niu Z. (2019), Tracking the Spatial-Temporal Evolution of Carbon Emissions in China from 1999 to 2015: A Land Use Perspective,*Sustainability*, **11**, 1-27. https://doi.org/10.3390/su11174531

Wang X.Jand Cheng Y. (2020), Research on the influencing mechanism of urbanization on carbon emission efficiency——Based on an empirical study of 118 countries, *World Regional Studies*, **29**, 503-511.

Wang X.M., Wu J., Wang Z., Jia X.T. and Bai B. (2020), An Accounting of CO_2 Emission in Chinese

418 Cities and Spatial Pattern Analysis, *Urban and Environmental Studies*, **01**, 67-80.
419 Wang Y. and He Y.F. (2019), A study on the relationship between carbon emissions and economic
420 development in the central region of western China: a case of Xi'an City, *Ecological Science*, **38**,
421 217-224.
422 Wang Y., Luo X., Chen W., Zhao M. and Wang B. (2019), Exploring the spatial effect of urbanization
423 on multi-sectoral CO_2 emissions in China, *Atmospheric Pollution Research*, **10**,1610-1620.
424 https://doi.org/10.1016/j.apr.2019.06.001
425 Wang Y.N., Xie Y.Q., Xie L.Q. and Chen W. (2019), Factor Decomposition of Chinese Urban
426 Household Carbon Emissions-Empirical Analysis based on LMDI Model and Q-Clustering,
427 *Research of Environmental Sciences*, **32**, 539-546.
428 Wang Y.Q., Tang D.M., Zhang J.T., Meng N., Han B.L. and Ouyang Z.Y. (2020), The impact of
429 urbanization on carbon emission: Analysis of panel data from 158 cities in China, *Acta ecologica*
430 *sinica*, **40**, 7897-7907.
431 Wei Y.R. and Chen S.L. (2021). Spatial correlation and carbon balance zoning of land use carbon
432 emissions in Fujian Province, *Acta ecologica sinica*, **41**, 5814-5824.
433 Xu X., Ou J., Liu P., Liu X. and Zhang H. (2021), Investigating the impacts of three-dimensional
434 spatial structures on CO_2 emissions at the urban scale, *Science of the Total Environment*, **762,**1-
435 11. https://doi.org/10.1016/j.scitotenv.2020.143096
436 Xu Z., Li C. and Niu L. (2022), Decoupling Relationship Between Land Mixed Use and Carbon
437 Emissions in Hohhot-Baotou-Ordos-Yulin Urban Agglomeration, *Research of Environmental*
438 *Sciences*,**35**, 299-308.
439 Yang H.R. and Wu Q. (2021), Dynamic Simulation of Carbon Emissions from Land Use in Nanjing
440 City under Different Policy Scenarios, *Areal research and development*, **40**, 121-126.
441 Zhang P.F., Hu Y.M and Xiong Z.P. (2014), Extraction of Three-Dimensional Architectural Data from
442 QuickBird Images, *Journal of the Indian Society of Remote Sensing,* **42**(2): 409-416.
443 Zhang P.F. (2015), Spatiotemporal Features of the Three-Dimensional Architectural Landscape in

Qingdao, China, *PLOS ONE*, **10**(9): 1-13.

Zhang S., Li Z., Ning X. and Li L. (2021), Gauging the impacts of urbanization on CO_2 emissions from the construction industry: Evidence from China, *Journal of Environmental Management*, **288**,1-12. https://doi.org/10.1016/j.jenvman.2021.112440

Zhang Y.N. and Pan J.H. (2019), Spatio-temporal simulation and differentiation pattern of carbon emissions in China based on DMSP/OLS nighttime light data, *China Environmental Science*, **39**, 1436-1446.

Zhao M.X., Lu L.H., Zhang B.L. and Luo H. (2021), Dynamic Relationship Among Energy Consumption，Economic Growth and Carbon Emissions in China, *Research of Environmental Sciences*, **34**, 1509-1522.

Zheng Y., Lu F., Liu J.R. and Wang X.K. (2020), Comparative study on CO_2 emissions from fossil energy consumption and its influencing factors in typical cities of China, *Acta ecologica sinica,* **40**, 3315-3327.

Zhou M.D., Kuang Y.Q. and Yun G.L. (2020), Analysis of Driving Factors of Atmospheric PM2.5 Concentration in Guangzhou City Based on Geo-Detector, *Research of Environmental Sciences*, **33**, 271-279.